

Electrocoagulation Process for Chromium Removal in Leather Tanning Effluents

Etih Hartati^{1*}, Lina Hasyati¹, Didin Agustin Permadi¹,
Djaenudin², Dani Permana³, Herlian Eriska Putra^{2,4}

¹ Faculty of Civil Engineering and Planning, Division of Environmental Engineering, Institut Teknologi Nasional, Bandung, 40124, Indonesia

² Research Center for Environmental and Clean Technology, The National Research and Innovation of the Republic of Indonesia (BRIN), Bandung Advanced Science and Creative Engineering Space (BASICS), Kawasan Sains dan Teknologi (KST) Prof. Dr. Samaun Samadikun, Jalan Cisitu-Sangkuriang No. 21 D, Bandung, 40135, Indonesia

³ Research Center for Genetic Engineering, the National Research and Innovation Agency of the Republic of Indonesia (BRIN), Kawasan Sains dan Teknologi (KST) Ir. Soekarno, Jalan Raya Jakarta-Bogor, KM. 46, Cibinong, Bogor, 16911, Indonesia

⁴ Collaborative Research Center for Zero Waste and Sustainability, Widya Mandala Surabaya Catholic University, Surabaya, 60114, Indonesia

* Corresponding author's e-mail: etih@itenas.ac.id

ABSTRACT

The application of chromium sulfate in tanning operations yields chromium-laden wastewater, posing significant environmental risks. This research explored electrocoagulation as a remedial measure for tannery effluents. Varied parameters – pH (4, 7, 10), electric currents (0.5, 1.0, 1.5 A), and durations (1, 2, 3 h) – were optimized to diminish the chromium content. Evaluation based on initial and final chromium concentrations demonstrated 99.94% removal efficiency at pH 4, 1.5 A, over 3 hours. Achieving the 0.6 mg/L target concentration occurred at pH 4, 0.91 A, for 3 hours. This study highlighted the effectiveness of electrocoagulation in chromium mitigation within tannery wastewater, showcasing its potential as an environmentally sustainable remediation.

Keywords: wastewater, leather tanning industry, electrocoagulation, chromium, removal efficiency.

INTRODUCTION

Tanning, a process applied to raw animal skins and hides for leather production, serves to safeguard leather against microbial degradation, heat, and moisture (Bacardit et al., 2014; Sivakumar, 2022; Wu et al., 2020). Chromium (Cr), extensively utilized across industries like printed circuit board manufacturing, metal processing, electroplating, and metal finishing (Guertin et al., 2016), prominently features in many leather tanning procedures using chromium sulfate (Tejada Tovar et al., 2021). Nevertheless, the surplus chromium sulfate in wastewater poses a critical issue due to chromium (Cr) being a hazardous heavy

metal (Prasad et al., 2021; Tamjidi and Esmacili, 2019). The toxicity of a heavy metal correlates with its ion valence; for instance, Cr⁶⁺ exhibits approximately 100 times greater toxicity than Cr³⁺, along with its highly corrosive and carcinogenic nature (Abdulmalik et al., 2023; DesMarias and Costa, 2019; Song et al., 2024). Furthermore, the exposure to Cr heavy metals can lead to dermatitis and, in cases of excessive uptake, trigger rhinitis (Bandara et al., 2020). Understanding these implications is crucial in addressing the environmental and health impacts of chromium residues in tannery effluents.

Various methods are employed to mitigate chromium contamination in wastewater, including

adsorption (Hashem et al., 2024; Madhusudan et al., 2023; Masood et al., 2023), reverse osmosis (Bratovic et al., 2022; George et al., 2015; Pan et al., 2023), chemical precipitation (Bratovic et al., 2022; George et al., 2015; Hosseine Amirhandeh et al., 2022), and oxidation-reduction processes (Wang et al., 2018; Zhang et al., 2023). Adsorption entails the use of materials like activated carbon or zeolite to absorb chromium, necessitating periodic replacement and incurring higher operational costs. Reverse osmosis relies on pressure and consumes substantial energy to separate chromium, while chemical precipitation using additives like iron sulfate or calcium hydroxide may elevate the chemical waste levels. Oxidation-reduction processes transform chromium into less hazardous forms but often require additional treatment steps. However, electrocoagulation stands out for its selective targeting of suspended particles, yielding larger, stable flocs and minimal sludge production (Deghles and Kurt, 2017a; Moussa et al., 2017), demonstrating the substantial potential for efficient chromium reduction while ensuring an environmentally friendly approach, especially relevant in industries like leather tanning.

The electrocoagulation process occurs within an electrolysis vessel fitted with electrodes (cathode and anode) facilitating direct electric current conduction, immersed in the wastewater serving as an electrolyte. The applied electrical energy at the anode induces the dissolution of aluminum into the solution, reacting subsequently with hydroxyl ions from the cathode, forming aluminum hydroxide. This compound initiates coagulation and flocculation processes, effectively eliminating suspended particles from the wastewater (Afiatun et al., 2019). Essential parameters influencing electrocoagulation efficacy encompass voltage, duration, wastewater pH, and the conductivity of the electrocoagulation reactor and electrodes (Xu et al., 2019).

In Indonesia, the majority of small-scale leather tanning industries, managed by local communities, grapple with challenges in treating chromium-containing waste (Deghles and Kurt, 2017b). Traditional treatment methods, such as precipitation and chemical coagulation, have limitations in achieving efficient chromium removal. These issues persist due to the prevalent use of PAC (poly aluminum chloride) and PAS (poly aluminum sulfate), known for their poor stability, limited coagulation efficiency,

and sluggish floc formation time (Astuti et al., 2022; Aziz et al., 2017; Nti et al., 2021). Moreover, the utilization of PAC contributes to the presence of toxic Al^{3+} in processed water, posing potential hazards (Simbarta Tarigan et al., 2021). Despite these remedies, their widespread adoption in wastewater treatment may still lead to residual sludge and environmental concerns, emphasizing the urgency to explore more efficient and eco-friendly alternatives like electrodeposition technology within these smaller-scale industrial setups. The electrocoagulation process, however, stands out as an innovative and sustainable alternative.

The existing literature lacks an in-depth exploration of the electrocoagulation process specifically tailored for chromium removal in leather tanning effluents. While conventional methods have been employed, their limitations in terms of efficiency and environmental impact necessitate the exploration of novel technologies. The conducted study addressed this research gap by providing a detailed investigation into the electrocoagulation process, evaluating its performance, and identifying areas where it surpasses conventional techniques. In this study, electrocoagulation optimized parameters such as pH, electric current, and time to effectively remove residual Cr from the treated wastewater. The primary aim of the study was to assess the cost-efficiency of the electrocoagulation process in treating wastewater derived from the leather tanning industry, focusing on optimal pH, electric current, and detention time conditions. The emphasis of the treatment is on chromium, a heavy metal, correlating it with the best operational parameters through a statistical approach using Response Surface Methodology (RSM). This approach is anticipated to offer guidance in selecting the most suitable operational conditions for treating similar types of wastewater.

MATERIAL AND METHOD

Characterization of wastewater from home-based leather tanning industries

The tannery wastewater used in this study was sourced from a home-based facility located in Cianjur, West Java, Indonesia. Samples were directly collected from the influent wastewater channel within the facility and subsequently

stored in polypropylene bottles at 4°C until further analysis. The wastewater samples collected originated from the inlet of the wastewater treatment. The quantity of samples procured was aligned with the number of experiments conducted. Given the presence of 27 variations, the number of experiments performed corresponded to 27 trials. Each trial necessitated the use of 1,000 ml of sample, culminating in a total required sample volume of 27 liters. The original characteristics of the home-based tannery wastewater included a temperature of 25.1°C, pH at 25.1°C of 8.31, and a Cr⁶⁺ concentration of 245.1 mg/L.

Electrode and reactor preparation

The electrodes utilized in this study were derived from aluminum plates. Electrode preparation involved the following steps: 1) aluminum plates were cut into dimensions of 6 cm x 15 cm; 2) the electrodes were cleansed using acetone; 3) the aluminum plates were heated to a temperature of 105°C for 1 hour in an oven and then weighed to attain a consistent weight; and 4) the aluminum plates were stored in a desiccator until their use in the electrocoagulation experiments.

The study employed a batch system. The reactor utilized can be seen in Figure 1. The preparatory stages for the electrocoagulation reactor were as follows: 1) the prepared aluminum plates were placed with a 4 cm gap on a support structure. The distance between electrodes affects the electrolyte resistance—larger distances result in higher resistance, thereby reducing the flow of current; 2) one aluminum plate was connected

to the negative pole (cathode), and another prepared aluminum plate was linked to the positive pole (anode) via an ammeter connected to a rectifier; and 3) the electrodes were placed in a 1-liter chemical glass serving as the reactor, containing 1 liter of wastewater.

Experimental design

The experiment setup was structured utilizing statistical software. Optimization modeling employed the Box-Behnken Design (BBD) for optimum conditions. BBD encompassed 27 experimental sets, conducted in duplicate. Key independent variables including the pH, electric current (EC), and duration were systematically adjusted to optimize the electrocoagulation process for maximum Cr removal efficiency. Concurrently, efforts were made to identify the factors related to cost efficiency. An operational cost analysis was conducted to determine the expenses incurred during the electrocoagulation process. Within this study, the operational cost calculation focused solely on evaluating the energy consumption and electrode consumption. The ranges for initial pH, current density, and EC time spanned 4–10, 0.5–1.5 (A), and 1–3 hours, respectively, as depicted in Table 1. The outcomes of the process were represented as the percentage of removal, calculated using Equation 1.

$$\% R = \frac{C_{in} - C_{out}}{C_{in}} \times 100\% \quad (1)$$

where: % R – Removal (%); C_{in} – Concentration inlet (mg/L); C_{out} – Concentration outlet (mg/L).

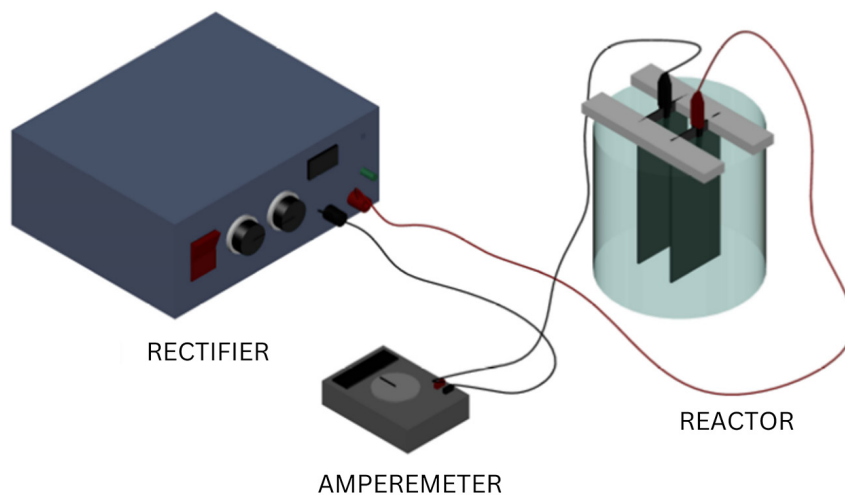


Figure 1. Electrocoagulation apparatus

The response variable (Y) obtained was subsequently analyzed using Minitab 17, resulting in a linear model tested for significance (p-value) and regression model adequacy (lack of fit). During the process optimization stage, each response had its optimization goals set within the software. This program conducted optimization based on the entered variable data and response measurements. The output from the optimization stage provided recommendations for several new optimal formulas according to the program. The objective of optimization was to seek the best conditions that reconcile all objective functions.

RESULTS AND DISCUSSION

pH variations during the electrocoagulation process

In the meticulous exploration of the electrocoagulation process, deliberate adjustments to the pH levels of wastewater samples were orchestrated at three distinct points: 4, 7, and 10. Fig. 1 clearly illustrates the dynamic shifts in pH over the course of the electrocoagulation, providing a comprehensive view of the intricate interplay between pH variations and the electrochemical processes involved. After 3 hours, a discernible surge in the wastewater pH was observed. This elevation is attributed to the liberation of OH⁻ ions and H₂ gas facilitated by the cathodic reaction. The degree of pH modulation is intricately connected to the cathode current density and the extent of Al³⁺ hydrolysis (Monteiro et al., 2022). The electrocoagulation process unfolds as a sequence of oxidation and reduction steps. Specifically, at the anode, H⁺ is generated by the oxidation of H₂O, while at the cathode, OH⁻ is produced through the reduction of H₂O. Notably, elevating the pH value results in a more pronounced increase in the production of OH⁻ ions compared to H⁺ ions (Aljaberi et al., 2022). This highlights the profound influence of meticulous pH control in fine-tuning the overall efficiency of the electrocoagulation process. This intricate interplay between pH adjustments and electrocoagulation emphasizes the significance of meticulous pH control to fine-tune the overall efficiency of the process. The complex relationship between cathode reactions, current density, and hydrolysis underscores the need for a profound comprehension of these factors to refine the accuracy and effectiveness of electrocoagulation in wastewater treatment.

Table 1. Experimental design of electrocoagulation process of tannery wastewater

Run	Factor 1 Initial pH	Factor 2 Current (Ampere)	Factor 3 Time (hour)
1	4	0.5	1
2	4	0.5	2
3	4	0.5	3
4	4	1.0	1
5	4	1.0	2
6	4	1.0	3
7	4	1.5	1
8	4	1.5	2
9	4	1.5	3
10	7	0.5	1
11	7	0.5	2
12	7	0.5	3
13	7	1.0	1
14	7	1.0	2
15	7	1.0	3
16	7	1.5	1
17	7	1.5	2
18	7	1.5	3
19	10	0.5	1
20	10	0.5	2
21	10	0.5	3
22	10	1.0	1
23	10	1.0	2
24	10	1.0	3
25	10	1.5	1
26	10	1.5	2
27	10	1.5	3

Temperature changes during the electrocoagulation process

In the realm of liquid waste processing, temperature emerges as a pivotal determinant influencing chemical reactions. The temperature fluctuations of liquid waste under treatment hinge on variables, such as pH, current strength, and processing duration. A visual representation of these temperature dynamics is portrayed in Figure 3, which delineates the shifts occurring during the electrocoagulation process. As Figure 3 illustrates, the electrocoagulation process triggers a temperature surge ranging from 23°C to 38°C. The apex of this temperature increase materializes at an electrical current of 1.5 Amperes and a pH level of 4. Noteworthy are the direct correlation

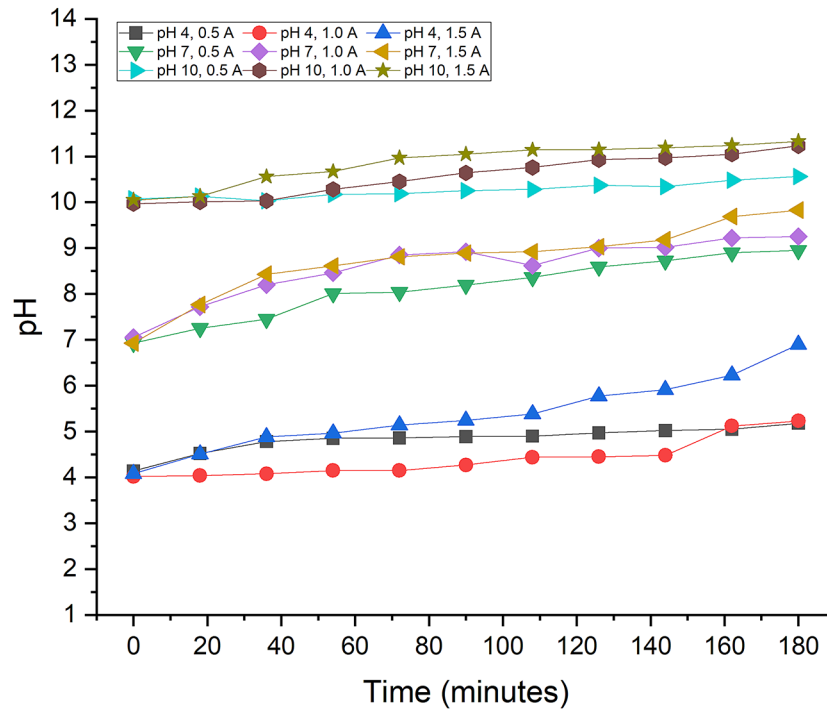


Figure 2. Changes to pH over time

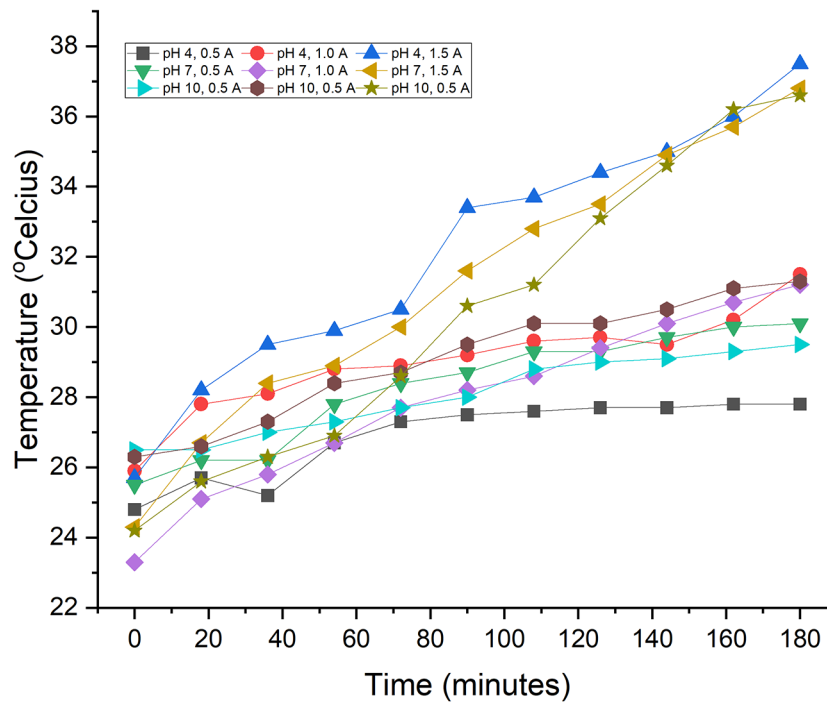


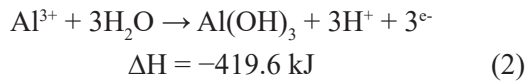
Figure 3. Changes to pH over time

between higher electrical currents and more pronounced temperature spikes. The temperature elevation during electrocoagulation is instigated by the release of Al^{3+} metal hydroxide ions. This liberation prompts a pH elevation in the electrocoagulation process, unleashing heat energy that

exerts an influential effect on the reaction rate (Cai et al., 2022; Dakhem et al., 2022).

Consequently, protracted electrocoagulation periods can yield a substantial escalation in temperature due to the sustained release of heat energy. This phenomenon emanates from the diverse reactions

intrinsic to electrocoagulation, encompassing electrolysis, hydrolysis, and redox reactions, all of which yield heat as a byproduct (López-Guzmán et al., 2021; Winoto et al., 2020). The underlying chemical process is encapsulated in the Eq. 2.



The negative ΔH reaction value (-419.6 kJ) signifies the exothermic nature of the reaction. Exothermic reactions emit heat, which dissipates into the surrounding environment, elevating the solution temperature (Ullah, 2021). The heat generated has the potential to raise the temperature of the wastewater, thereby influencing both the efficacy of the treatment process and the quality of the final effluent (Wang et al., 2022). Consequently, meticulous monitoring and regulation of temperature throughout the electrocoagulation process become imperative, ensuring optimal performance, and mitigating potential adverse environmental impacts (Mao et al., 2023).

Electrode mass changes in the electrocoagulation process

As the electric current was elevated, there was a corresponding increase in the oxidation of aluminum (Al). The anodic oxidation led to the dissolution of Al^{3+} cations in the water (Benea et al., 2022). Figure 4 illustrates the theoretically anticipated reduction in Al mass. The data depicted

in Figure 4 highlight the disparities between theoretical calculations and actual outcomes. Notably, the actual reduction in anode mass was found to be lower than the theoretically predicted values. This diminution in anode mass can be attributed to multiple factors, including energy conversion into heat, current loss due to the resistance of connecting materials, and the quality of the anode material (Meng et al., 2020).

The heightened reduction in electrode mass was particularly pronounced in electrocoagulation processes conducted with elevated currents. The data on electrode mass reduction serve as a valuable metric for estimating the optimal electrode replacement time. Further insights into the comparative conditions of aluminum—pre-usage, usage as a cathode, and usage as an anode—are elucidated in Figure 5. This comparative analysis sheds light on the evolving state of the aluminum electrodes throughout the electrocoagulation process, providing valuable information for optimizing operational parameters and enhancing the efficiency of the electrocoagulation system.

Wastewater quality analysis

Prior to the application of electrocoagulation, the chromium (Cr) content in the wastewater sample measured 245.1 mg/L. Subsequently, the Cr content exhibited variations based on factors such as pH, electric current, and duration, as depicted in Figures 6–8. Electrocoagulation, illustrated in

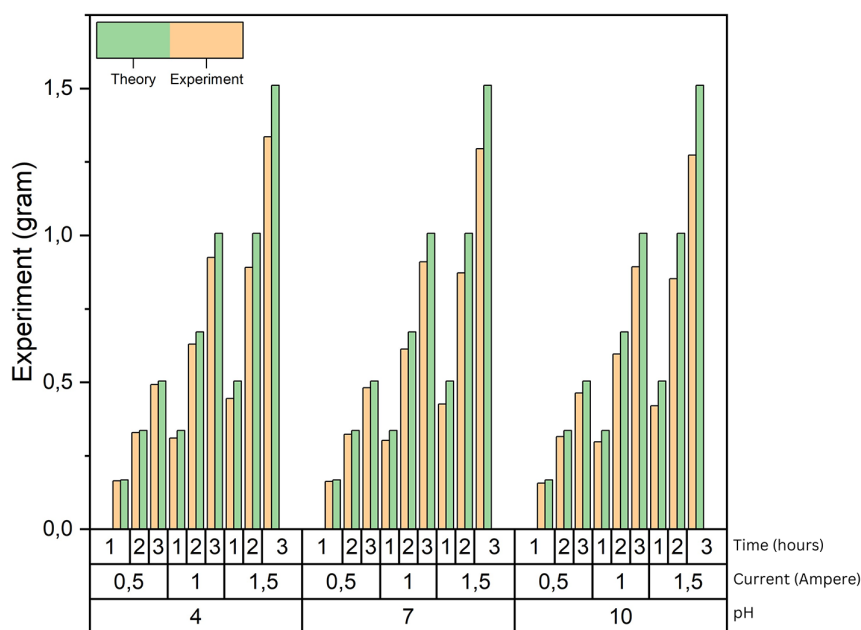


Figure 4. Anode mass reduction

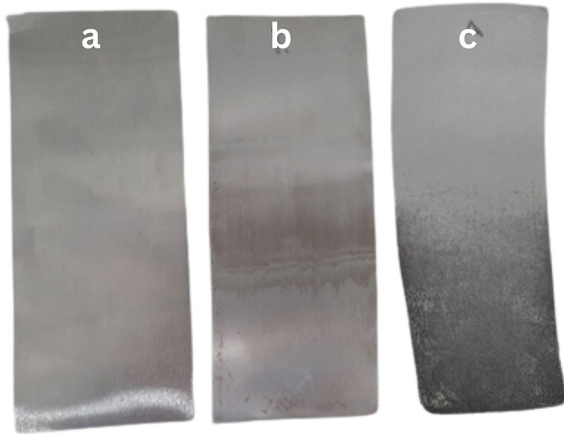
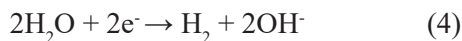


Figure 5. Electrode comparison: (a) aluminum plate before use, (b) aluminum plate as cathode, (c) aluminum plate as the anode

Figures 6–8, demonstrated a notable decrease in Cr content. The electrochemical reactions occurring at the anode and cathode were described by the Equations 3 and 4. (Suyati et al., 2019):

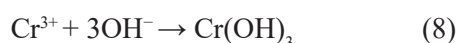
At the anode:



At the anode, aluminum (Al) metal dissolved to form Al^{3+} ions, subsequently hydrolyzing to produce solid $\text{Al}(\text{OH})_3$, a water-insoluble substance. $\text{Al}(\text{OH})_3$ functioned as a coagulant within the electrocoagulation cell, participating in the coagulation-flocculation process. The reaction sequence involved the formation of $\text{Al}(\text{OH})_3$ and H^+ ions, followed by the generation of $\text{Al}(\text{OH})_4^-$ ions (Zaied et al., 2020), which facilitated Cr removal:

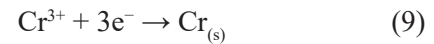


The formed $\text{Al}(\text{OH})_4^-$ ions aided in binding to Cr, promoting the removal of Cr from the wastewater through the formation of $[\text{Cr}(\text{Al}(\text{OH})_4)_3]_s$. Additionally, the decrease in Cr content resulted from the precipitation of $\text{Cr}(\text{OH})_3$ due to the interaction between Cr in the wastewater and OH^- ions:



The $\text{Cr}(\text{OH})_3$ precipitate served as an electro-positive floc core, attracting excess OH^- ions and forming flocs of $\text{Cr}(\text{OH})_4^-$, which, in turn, attracted other metal cations present in the wastewater (Boinpally et al., 2023). At the cathode, Cr^{3+} was

reduced to solid (Zaied et al., 2020), attaching to the cathode rod:



Concurrently, the H_2 gas production occurred at the cathode, leading to the ascent of dirt formed in the wastewater to the surface. The production of H_2 gas was accompanied by the formation of hydroxide ions, which bound to pollutants and formed non-dissolvable compounds that floated to the reactor surface (Ali Maitlo et al., 2019). The reduction in the Cr content was particularly pronounced under acidic conditions (pH 4), as observed in Figures 6-8, with the optimal reaction occurring at pH 4 compared with neutral (pH 7) and base conditions (pH 10) at different electrical current. The larger the electric current strength used, the greater the chromium concentration that can be removed. To achieve acidic conditions, sulfuric acid (H_2SO_4) was added, dissociating at the cathode:



Under acidic conditions, H_2 gas production increased through H^+ reduction:



The enhanced production of H_2 gas resulted in greater amounts of the contaminant floating on the surface and increased Cr separation from the wastewater. Prolonging the electrocoagulation process further amplified the separation of metal ions (Zaied et al., 2020). As depicted in Figures 4–6, an increase in process time correlated with a decrease in the Cr content, attributed to the accelerated oxidation of Cr^{3+} and the formation of $\text{Cr}(\text{OH})_3$, generating small particles that formed settleable flocs (Hasan et al., 2021). The reduction in the Cr content was also influenced by the concentration of Al^{3+} cations in the wastewater, where a higher concentration led to increased cation absorption into the solution. In contrast to precipitation and chemical coagulation, electrocoagulation demonstrates superior performance in terms of chromium removal efficiency and operational flexibility. The process ensures the generation of stable and easily separable flocs, resulting in enhanced separation efficiency and reduced sludge volume.

The optimum condition of the electrocoagulation process

Response Surface Methodology (RSM) serves as a comprehensive set of statistical and mathematical tools for the enhancement and

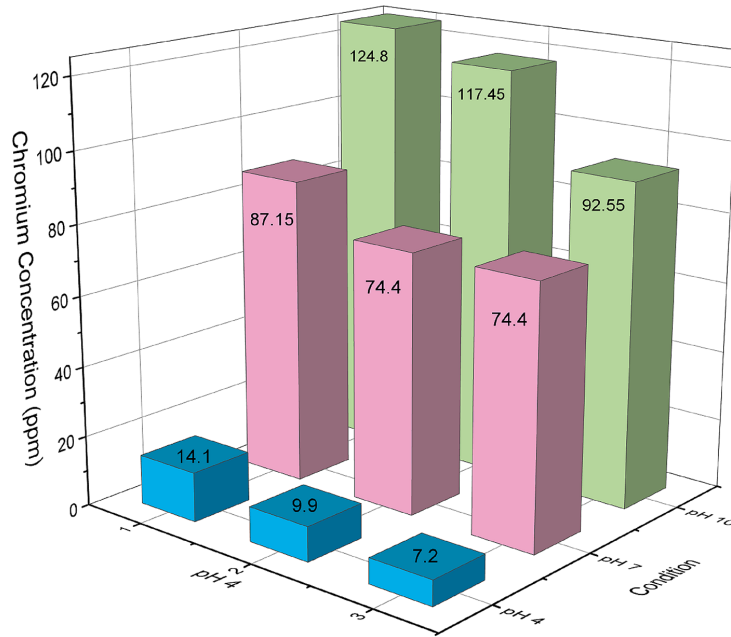


Figure 6. Chromium concentration at an electric current of 0.5 A

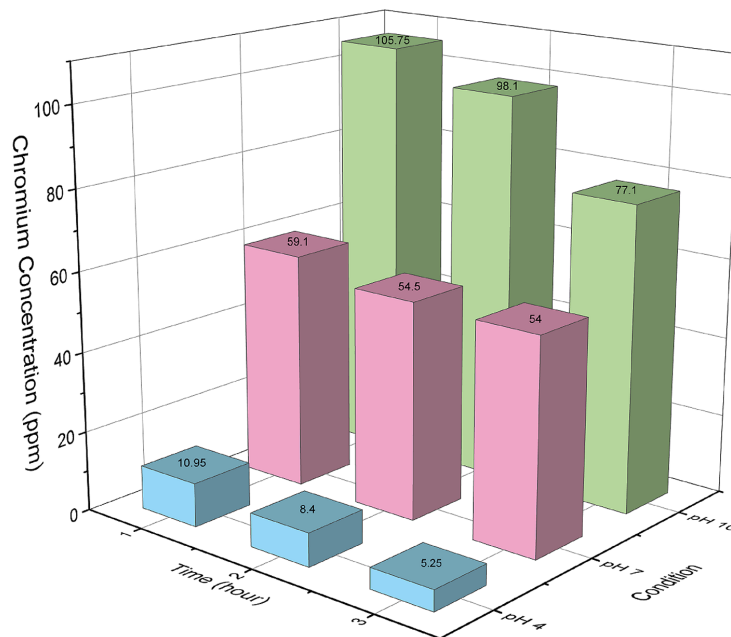


Figure 7. Chromium concentration at an electric current of 1 A

optimization of processes affected by various variables. This methodology involves the creation of a predictive model to evaluate the impact of individual variables on the response of interest (Dahish, 2023; Sulaiman et al., 2023). In the context of this study, RSM, executed through the Minitab 18 application, was employed to optimize the electrocoagulation parameters, specifically pH, electric current, and duration. The outcomes

indicated that both pH value and electric current significantly influenced chromium (Cr) content ($p < 0.05$), whereas the impact of time was found to be statistically insignificant ($p > 0.5$). Furthermore, the RSM results revealed that pH (x_1), electric current (x_2), and time (x_3) collectively influenced Cr content (y) with a high coefficient of determination ($R^2 = 0.96$), while other unidentified variables played a minor role ($R^2 = 0.04$). The

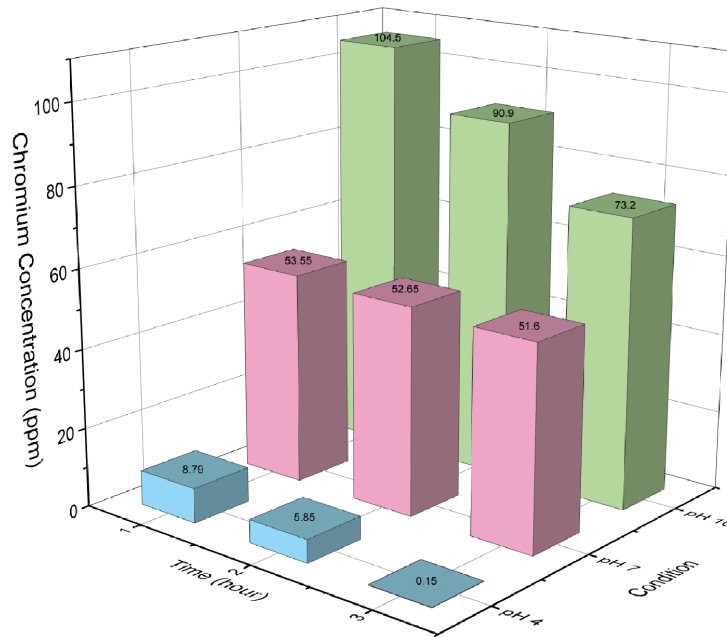


Figure 8. Chromium concentration at an electric current of 1.5 A

optimization of parameters was undertaken utilizing RSM and the Minitab application (Lamidi et al., 2023). The RSM equation derived for optimal electrocoagulation is expressed as follows:

$$y = -37.7 + 29.28 x_1 - 49.2 x_2 - 28.2 x_3 - 1.031 x_{12} + 21.7 x_{22} + 3.70 x_{32} - 2.71 x_1 \times x_2 + 1.477 x_1 \times x_3 + 3.53 x_2 \times x_3 \quad (12)$$

where: y represents the Cr concentration (mg/L), x_1 denotes pH, x_2 represents electric current (A), and x_3 corresponds to time (h).

Figure 9 illustrates that electrocoagulation conducted at pH 4, an electric current of 1.29 A, and a duration of 2.07 h resulted in a substantial reduction of the Cr content from 245.1 to 0.6 mg/L, signifying the most optimal conditions achieved through the optimization process.

Energy consumption, electrode consumption, and specific energy

Electrocoagulation presents several discernible advantages over conventional methods. Firstly, it facilitates the rapid and efficient removal of Cr^{3+} ions through the formation of insoluble metal hydroxide flocs. The process is adaptable to a diverse range of effluent characteristics and operates with relatively low energy consumption. Moreover, electrocoagulation minimizes the need for additional chemical reagents, thereby mitigating the overall environmental impact associated with treatment processes.

The analysis of energy consumption, electrode consumption, and specific energy in electrocoagulation for chromium removal under

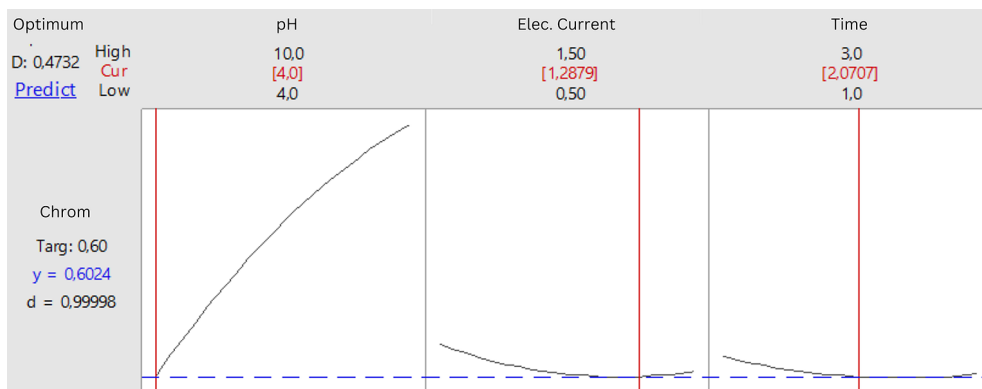


Figure 9. Optimal conditions for electrocoagulation taken from the RSM software

Table 2. Energy consumption, electrode consumption, and specific energy

Variance	Energy consumption (kWh/m ³)	Electrode consumption (kg/m ³)	Specific energy (kWh/kg Cr)
pH 4 - 0.5 A - 1 h	1.31	0.047	5.67
pH 4 - 0.5 A - 2 h	2.88	0.093	12.24
pH 4 - 0.5 A - 3 h	4.98	0.140	20.93
pH 4 - 1.0 A - 1 h	4.61	0.093	19.69
pH 4 - 1.0 A - 2 h	7.86	0.187	33.21
pH 4 - 1.0 A - 3 h	13.83	0.280	57.66
pH 4 - 1.5 A - 1 h	8.145	0.140	34.47
pH 4 - 1.5 A - 2 h	15.39	0.280	64.33
pH 4 - 1.5 A - 3 h	22.95	0.420	93.69
pH 7 - 0.5 A - 1 h	1.525	0.047	8.93
pH 7 - 0.5 A - 2 h	2.84	0.093	17.98
pH 7 - 0.5 A - 3 h	4.59	0.140	26.89
pH 7 - 1.0 A - 1 h	4.33	0.093	22.73
pH 7 - 1.0 A - 2 h	8.68	0.187	46.67
pH 7 - 1.0 A - 3 h	12.81	0.280	67.03
pH 7 - 1.5 A - 1 h	8.775	0.140	45.81
pH 7 - 1.5 A - 2 h	15.87	0.280	82.46
pH 7 - 1.5 A - 3 h	23.49	0.420	121.40
pH 10 - 0.5 A - 1 h	1.445	0.047	11.32
pH 10 - 0.5 A - 2 h	3.09	0.093	20.26
pH 10 - 0.5 A - 3 h	3.825	0.140	31.80
pH 10 - 1.0 A - 1 h	3.35	0.093	24.04
pH 10 - 1.0 A - 2 h	7.3	0.187	43.45
pH 10 - 1.0 A - 3 h	11.82	0.280	80.41
pH 10 - 1.5 A - 1 h	6.645	0.140	38.66
pH 10 - 1.5 A - 2 h	15.51	0.280	100.58
pH 10 - 1.5 A - 3 h	22.14	0.420	158.54

varying pH values, electric currents, and durations is presented in Table 1. The data in Table 1 illustrate a notable influence of time and electric current on both energy and electrode consumption. Specific energy, denoted in kilowatt-hours (kWh), represents the energy required to eliminate 1 kg of total Cr mass. A lower specific energy value indicates greater efficiency in the electrocoagulation process, thereby reducing the overall cost associated with the Cr removal from wastewater (Hasan et al., 2021). When examining the results it was found that the lowest specific energy of 5.67 kWh/kg Cr was achieved under conditions of pH 4, an electric current of 0.5 A, and a duration of 1 hour. However, these optimal parameters did not result in the desired reduction of the Cr content from 245.1 to 0.6 mg/L, failing to meet the quality standard. In contrast, the conditions of pH 4, an electric current of 1.28 A, and a duration of 2.07

hours led to a specific energy of 52.63 kWh/kg Cr. Meanwhile, the highest efficiency was observed at pH 4, an electric current of 1.5 A, and 3 hours, although this configuration demanded a substantial specific energy of 93.69 kWh/kg Cr due to the elevated electric current and extended duration. These findings underscore the intricate trade-off between achieving optimal efficiency and managing the associated energy costs in the electrocoagulation process for Cr removal.

CONCLUSIONS

In conclusion, the conducted study delved into the electrocoagulation process for chromium removal in leather tanning effluents, revealing its distinct advantages over conventional methods. Addressing a crucial research gap, the research

provided nuanced insights into the dynamic interplay of pH, temperature, and anode mass throughout the process. Notably, the study identified the pivotal role of initial pH, highlighting optimal efficiency at pH 4, an electric current of 1.5 A, and a duration of 3 hours, resulting in an impressive 99.94% reduction in the chromium content from 245.1 to 0.15 mg/L. Validating these findings, the Response Surface Methodology (RSM) indicated that a chromium concentration of 0.6 mg/L can be achieved at pH 4, an electric current of 1.29 A, and a duration of 2 hours. This meticulous parameter selection, guided by the electrocoagulation process, demonstrates its high effectiveness in chromium removal and offers crucial insights for sustainable and efficient wastewater treatment in the leather industry.

Acknowledgments

The authors would like to thank the LPPM Itenas for the international journal publication grant No.339/B.05/LP2M-Itenas/I/2020. The analysis in this work has been done using the facilities of ELSA BRIN, National Research and Innovation Agency of Indonesia (BRIN).

REFERENCES

- Abdulmalik, A.F., Yakasai, H.M., Usman, S., Muhammad, J.B., Jagaba, A.H., Ibrahim, S., Babandi, A., Shukor, M.Y., 2023. Characterization and invitro toxicity assay of bio-reduced hexavalent chromium by *Acinetobacter* sp. isolated from tannery effluent. *Case Studies in Chemical and Environmental Engineering* 8, 100459. <https://doi.org/10.1016/J.CSCEE.2023.100459>
- Afiatun, E., Pradiko, H., Fabian, E., 2019. Turbidity reduction for the development of pilot scale electrocoagulation devices. *International Journal of Geomate* 16, 123–128. <https://doi.org/10.21660/2019.56.4682>
- Ali Maitlo, H., Kim, K.H., Yang Park, J., Hwan Kim, J., 2019. Removal mechanism for chromium (VI) in groundwater with cost-effective iron-air fuel cell electrocoagulation. *Sep Purif Technol* 213, 378–388. <https://doi.org/10.1016/J.SEPPUR.2018.12.058>
- AlJaberi, F.Y., Alardhi, S.M., Ahmed, S.A., Salman, A.D., Juzsakova, T., Cretescu, I., Le, P.C., Chung, W.J., Chang, S.W., Nguyen, D.D., 2022. Can electrocoagulation technology be integrated with wastewater treatment systems to improve treatment efficiency? *Environ Res* 214, 113890. <https://doi.org/10.1016/J.ENVRES.2022.113890>
- Astuti, D., Wedaning, A., Janametri, A., Darnoto, S., Asyfiradayati, R., 2022. Reduction of chromium levels in tanning wastewater by phytoremediation method: a review. *International Journal Of Multi-science*, 3(1), 34-53.
- Aziz, N., Effendy, N., Basuki, K.T., 2017. Comparison of poly aluminium chloride (pac) and aluminium sulphate coagulants efficiency in waste water treatment plant, *Jurnal Inovasi Teknik Kimia*, 2, 24–31. <http://dx.doi.org/10.31942/inteka.v2i1.1738>
- Bacardit, A., Van Der Burgh, S., Armengol, J., Ollé, L., 2014. Evaluation of a new environment friendly tanning process. *J Clean Prod*, 65, 568–573. <https://doi.org/10.1016/J.JCLEPRO.2013.09.052>
- Bandara, A.B.P., Kumara, G.M.P., Matsuno, A., Saito, T., Nga, T.T.V., Kawamoto, K., 2020. Examination of crushed laterite brick for removal of chromium and arsenic from wastewater. *International Journal of GEOMATE*, 19, 22–30. <https://doi.org/10.21660/2020.74.9176>
- Benea, L., Simionescu – Bogatu, N., Chiriac, R., 2022. Electrochemically obtained Al₂O₃ nanoporous layers with increased anticorrosive properties of aluminum alloy. *Journal of Materials Research and Technology*, 17, 2636–2647. <https://doi.org/10.1016/j.jmrt.2022.02.038>
- Boinpally, S., Kolla, A., Kainthola, J., Kodali, R., Vemuri, J., 2023. A state-of-the-art review of the electrocoagulation technology for wastewater treatment. *Water Cycle*, 4, 26–36. <https://doi.org/10.1016/J.WATCYC.2023.01.001>
- Bratovic, A., Buksek, H., Helix-Nielsen, C., Petrinc, I., 2022. Concentrating hexavalent chromium electroplating wastewater for recovery and reuse by forward osmosis using underground brine as draw solution. *Chemical Engineering Journal*, 431, 133918. <https://doi.org/10.1016/J.CEJ.2021.133918>
- Cai, D.-G., Qiu, C.-Q., Zhu, Z.-H., Zheng, T.-F., Wei, W.-J., Chen, J.-L., Liu, S.-J., Wen, H.-R., 2022. Fabrication and DFT Calculation of Amine-Functionalized Metal–Organic Framework as a Turn-On Fluorescence Sensor for Fe³⁺ and Al³⁺ Ions. *Inorg Chem*, 61, 14770–14777. <https://doi.org/10.1021/acs.inorgchem.2c02195>
- Dahish, H.A., 2023. Predicting the compressive strength of concrete containing crumb rubber and recycled aggregate using response surface methodology. *International Journal of GEOMATE*, 24, 117–124. <https://doi.org/10.21660/2023.104.3788>
- Dakhem, M., Ghanati, F., Afshar Mohammadian, M., Sharifi, M., 2022. Tea leaves, efficient biosorbent for removal of Al³⁺ from drinking water. *International Journal of Environmental Science and Technology*, 19, 10985–10998. <https://doi.org/10.1007/s13762-022-04313-6>
- Deghles, A., Kurt, U., 2017a. Hydrogen Gas

- Production from Tannery Wastewater by Electrocoagulation of a Continuous Mode with Simultaneous Pollutants Removal. *IOSR Journal of Applied Chemistry*, 10, 40–50. <https://doi.org/10.9790/5736-1003014050>
16. Deghles, A., Kurt, U., 2017b. Hydrogen Gas Production from Tannery Wastewater by Electrocoagulation of a Continuous Mode with Simultaneous Pollutants Removal. *IOSR Journal of Applied Chemistry*, 10, 40–50. <https://doi.org/10.9790/5736-1003014050>
17. DesMarias, T.L., Costa, M., 2019. Mechanisms of chromium-induced toxicity. *Curr Opin Toxicol*, 14, 1–7. <https://doi.org/10.1016/J.COTOX.2019.05.003>
18. George, J.S., Ramos, A., Shipley, H.J., 2015. Tanning facility wastewater treatment: Analysis of physical–chemical and reverse osmosis methods. *J Environ Chem Eng*, 3, 969–976. <https://doi.org/10.1016/J.JECE.2015.03.011>
19. Guertin, J., Jacobs, J., Avakian, C.P., 2016. Chromium(VI) Handbook, Chromium(VI) Handbook.
20. Hasan, M.A., Hashem, M.A., Arman, M.N., Momen, M.A., 2021. Batch Electrocoagulation Process for Removal of Chromium from Tannery Wastewater. *Journal of Engineering Science*, 12, 29–34. <https://doi.org/10.3329/jes.v12i1.53098>
21. Hashem, Md.A., Mim, M.W., Noshin, N., Maoya, M., 2024. Chromium adsorption capacity from tannery wastewater on thermally activated adsorbent derived from kitchen waste biomass. *Cleaner Water*, 1, 100001. <https://doi.org/10.1016/J.CLWAT.2023.100001>
22. Hosseine Amirhandeh, S.Z., Salem, A., Salem, S., 2022. Sono-chemical extraction of silica from rice husk for uptake of chromium species from tannery wastewater: Effect of aging time on porous structure. *Mater Lett*, 327, 132933. <https://doi.org/10.1016/J.MATLET.2022.132933>
23. Lamidi, S., Olaleye, N., Bankole, Y., Obalola, A., Aribike, E., Adigun, I., 2023. Applications of Response Surface Methodology (RSM) in Product Design, Development, and Process Optimization, in: *Response Surface Methodology - Research Advances and Applications*. IntechOpen. <https://doi.org/10.5772/intechopen.106763>
24. López-Guzmán, M., Flores-Hidalgo, M.A., Reynoso-Cuevas, L., 2021. Electrocoagulation process: An approach to continuous processes, reactors design, pharmaceuticals removal, and hybrid systems—a review. *Processes*. <https://doi.org/10.3390/pr9101831>
25. Madhusudan, P., Lee, C., Kim, J.O., 2023. Synthesis of Al₂O₃@Fe₂O₃ core-shell nanorods and its potential for fast phosphate recovery and adsorption of chromium (VI) ions from contaminated wastewater. *Sep Purif Technol*, 326, 124691. <https://doi.org/10.1016/J.SEPPUR.2023.124691>
26. Mao, Y., Zhao, Y., Cotterill, S., 2023. Examining Current and Future Applications of Electrocoagulation in Wastewater Treatment. *Water (Switzerland)*. <https://doi.org/10.3390/w15081455>
27. Masood, N., Irshad, M.A., Nawaz, R., Abbas, T., Abdel-Maksoud, M.A., AlQahtani, W.H., AbdElgawad, H., Rizwan, M., Abeer, A.H.A., 2023. Green synthesis, characterization and adsorption of chromium and cadmium from wastewater using cerium oxide nanoparticles; reaction kinetics study. *J Mol Struct*, 1294, 136563. <https://doi.org/10.1016/J.MOLSTRUC.2023.136563>
28. Meng, X., Xu, Y., Cao, H., Lin, X., Ning, P., Zhang, Y., Garcia, Y.G., Sun, Z., 2020. Internal failure of anode materials for lithium batteries — A critical review. *Green Energy & Environment*, 5, 22–36. <https://doi.org/10.1016/J.GEE.2019.10.003>
29. Monteiro, M.C.O., Dattila, F., López, N., Koper, M.T.M., 2022. The Role of Cation Acidity on the Competition between Hydrogen Evolution and CO₂ Reduction on Gold Electrodes. *J Am Chem Soc*, 144, 1589–1602. <https://doi.org/10.1021/jacs.1c10171>
30. Moussa, D.T., El-Naas, M.H., Nasser, M., Al-Marri, M.J., 2017. A comprehensive review of electrocoagulation for water treatment: Potentials and challenges. *J Environ Manage*, 186, 24–41. <https://doi.org/10.1016/J.JENVMAN.2016.10.032>
31. Nti, S.O., Buamah, R., Atebiya, J., 2021. Polyaluminium chloride dosing effects on coagulation performance: case study, barekese, ghana. *Water Pract Technol*, 16, 1215–1223. <https://doi.org/10.2166/wpt.2021.069>
32. Pan, Z., Yang, X., Liang, Y., Lyu, M., Huang, Y., Zhou, H., Wen, G., Yu, H., He, J., 2023. Chromium-containing wastewater reclamation via forward osmosis with sewage sludge ash temperature-sensitive hydrogel as draw agent. *Journal of Water Process Engineering*, 51, 103422. <https://doi.org/10.1016/J.JWPE.2022.103422>
33. Prasad, S., Yadav, K.K., Kumar, S., Gupta, N., Cabral-Pinto, M.M.S., Rezanian, S., Radwan, N., Alam, J., 2021. Chromium contamination and effect on environmental health and its remediation: A sustainable approaches. *J Environ Manage*, 285, 112174. <https://doi.org/10.1016/J.JENVMAN.2021.112174>
34. Simbarta Tarigan, B., Atiek Rostika Noviyanti, dan, Raya Bandung-Sumedang Km, J., 2021. Composition of Polyaluminum Chloride with Hydroxyapatite and Its Application for Separation of Hexavalent Chromium Ions.
35. Sivakumar, V., 2022. Towards environmental protection and process safety in leather processing – A comprehensive analysis and review. *Process Safety and Environmental Protection*, 163, 703–726. <https://doi.org/10.1016/J.PSEP.2022.05.062>
36. Song, U., Pyo, K.S., Song, H.H., Lee, S. ryung, Kim, J., 2024. Environmental toxicity assessment of chromium

- (III) oxide nanoparticles using a phytotoxic, cytotoxic, and genotoxic approach. *Emerg Contam*, 10, 100293. <https://doi.org/10.1016/J.EMCON.2023.100293>
37. Sulaiman, S.M., Nugroho, G., Saputra, H.M., Djaenudin, Permana, D., Fitria, N., Putra, H.E., 2023. Valorization of Banana Bunch Waste as a Feedstock via Hydrothermal Carbonization for Energy Purposes. *Journal of Ecological Engineering*, 24, 61–74. <https://doi.org/10.12911/22998993/163350>
38. Suyati, L., Fadilah Nur, I.D., Widodo, D.S., Gunawan, Rahmanto, W.H., 2019. Electrosynthesis of Al(OH)₃ by Al(s)|KCl(aq)||KCl(s)|C(s) system, in: IOP Conference Series: Materials Science and Engineering. Institute of Physics Publishing. <https://doi.org/10.1088/1757-899X/509/1/012066>
39. Tamjidi, S., Esmaceli, H., 2019. Chemically Modified CaO/Fe₃O₄ Nanocomposite by Sodium Dodecyl Sulfate for Cr(III) Removal from Water. *Chem Eng Technol*. <https://doi.org/10.1002/ceat.201800488>
40. Tejada tovar, C. nahir, Villabona Ortíz, A., Contreras Amaya, R., 2021. Electrocoagulation as an Alternative for the Removal of Chromium (VI) in Solution. *Tecnura*, 25, 28–42. <https://doi.org/10.14483/22487638.17088>
41. Wang, G., Zhang, J., Liu, L., Zhou, J.Z., Liu, Q., Qian, G., Xu, Z.P., Richards, R.M., 2018. Novel multi-metal containing MnCr catalyst made from manganese slag and chromium wastewater for effective selective catalytic reduction of nitric oxide at low temperature. *J Clean Prod*, 183, 917–924. <https://doi.org/10.1016/J.JCLEPRO.2018.02.207>
42. Wang, J.Y., Kadier, A., Hao, B., Li, H., Ma, P.C., 2022. Performance optimization of a batch scale electrocoagulation process using stainless steel mesh (304) cathode for the separation of oil-in-water emulsion. *Chemical Engineering and Processing - Process Intensification*, 174, 108901. <https://doi.org/10.1016/J.CEP.2022.108901>
43. Winoto, H.P., Gunawan, D., Indarto, A., 2020. Efficient phosphate recovery from fertilizer wastewater stream through simultaneous Ca and F ions removal. *Agrochemicals Detection, Treatment and Remediation: Pesticides and Chemical Fertilizers*, 369–400. <https://doi.org/10.1016/B978-0-08-103017-2.00014-3>
44. Wu, X., Qiang, X., Liu, D., Yu, L., Wang, X., 2020. An eco-friendly tanning process to wet-white leather based on amino acids. *J Clean Prod*, 270, 122399. <https://doi.org/10.1016/J.JCLEPRO.2020.122399>
45. Xu, X., Huang, H., Zhang, Y., Xu, Z., Cao, X., 2019. Biochar as both electron donor and electron shuttle for the reduction transformation of Cr(VI) during its sorption. *Environmental Pollution*, 244, 423–430. <https://doi.org/10.1016/J.ENVPOL.2018.10.068>
46. Zaied, B.K., Rashid, M., Nasrullah, M., Zularisam, A.W., Pant, D., Singh, L., 2020. A comprehensive review on contaminants removal from pharmaceutical wastewater by electrocoagulation process. *Science of The Total Environment*, 726, 138095. <https://doi.org/10.1016/J.SCITOTENV.2020.138095>
47. Zhang, T., Wang, P., Li, Y., Bao, Y., Lim, T.-T., Zhan, S., 2023. Advances in dual-functional photocatalysis for simultaneous reduction of hexavalent chromium and oxidation of organics in wastewater. *Environmental Functional Materials*, 2, 1–12. <https://doi.org/10.1016/J.EFMAT.2023.05.001>